Pulmonary subsolid nodules: what radiologists need to know about the imaging features and management strategy

Hyungjin Kim, Chang Min Park, Jae Moon Koh, Sang Min Lee, Jin Mo Goo

ABSTRACT
Pulmonary subsolid nodules (SSNs) refer to pulmonary nodules with pure ground-glass nodules and part-solid ground-glass nodules. SSNs are frequently encountered in the clinical setting, such as screening chest computed tomography (CT). The main concern regarding pulmonary SSNs, particularly when they are persistent, has been lung adenocarcinoma and its precursors. The CT manifestations of SSNs help radiologists and clinicians manage these lesions. However, the management plan for SSNs has not previously been standardized. Recently, the Fleischner Society published recommendations for the management of incidentally detected SSNs. The guidelines reflect the new lung adenocarcinoma classification system proposed by the International Association for the Study of Lung Cancer, American Thoracic Society, and European Respiratory Society (IASLC/ATS/ERS) and include six specific recommendations according to the nodule size, solid portion and multiplicity. This review aims to increase the understanding of SSNs and the imaging features of SSNs according to their histology, natural course, possible radiologic interventions, such as biopsy, localization prior to surgery, and current management.

From the Department of Radiology (H.K., C.M.P. ✉ cmpark@ radiol.snu.ac.kr, S.M.L., J.M.G.), Seoul National University College of Medicine, and Institute of Radiation Medicine, Seoul National University Medical Research Center, Seoul, Korea; Cancer Research Institute (C.M.P., J.M.G.), Seoul National University, Seoul, Korea; Department of Pathology (J.M.K.), Seoul National University Hospital, Seoul, Korea.

A ground-glass nodule (GGN) is the morphologic description of a pulmonary nodule category on thin-section chest computed tomography (CT). During the past decade, the natural history, management strategy and long-term prognosis in the case of GGNs have attracted attention. Pure GGNs are defined as focal nodular areas of increased lung attenuation through which lung parenchymal structures, such as the pulmonary vessels or bronchial structures, can be observed (1). Part-solid GGNs are nodules that present with both ground-glass and solid components in which the underlying lung architecture cannot be visualized (1, 2). The term subsolid nodules (SSNs) includes both pure and part-solid GGNs. In the Early Lung Cancer Action Project (ELCAP) study, researchers revealed that the malignancy rate of SSNs (34%) was higher than that of solid nodules (7%) (3). The malignancy rate for part-solid GGNs was 63%, and the rate for pure GGNs was 18% (3). Histologically, persistent SSNs represent a spectrum of peripheral adenocarcinomas or the precursors, from atypical adenomatous hyperplasias (AAH) to invasive adenocarcinomas (4), although this sequential development hypothesis has not yet been confirmed. However, not all SSNs are malignant. In fact, SSNs include various histologic backgrounds including many benign conditions, such as focal interstitial fibrosis, eosinophilic pneumonia, thoracic endometriosis, and focal hemorrhage (5, 6). Nevertheless, in consideration of the significance of lung cancer, we focus on SSNs in relation to adenocarcinomas in this review.

CT-pathologic correlations of subsolid nodules

Since a study by Jang et al. (7) first revealed that bronchioloalveolar carcinomas (BACs), which is an obsolete term that has been replaced by adenocarcinoma *in situ* (AIS), can be observed as SSNs on CT, several CT-pathologic correlation studies have been performed. AAH is defined as a localized, small (usually ≤5 mm) proliferation of atypical type II pneumocytes and/or Clara cells lining the alveolar walls and respiratory bronchioles (8). AAH usually appears on a CT as a small well-defined oval or round pure GGN ≤5 mm in diameter (Fig. 1), although these lesions have been reported to be as large as 1 to 2 cm (9, 10). Nonmucinous AIS typically appears as pure GGNs (Fig. 2), but a lesion with focal collapsed alveoli or focal thickened alveolar septa may manifest as a part-solid GGN (11). Mucinous AIS can appear as a solid nodule or as a consolidation (11).

Minimally invasive adenocarcinomas (MIAs), which is a newly introduced category in lung adenocarcinoma classification, are small, solitary adenocarcinomas (≤3 cm), with a predominantly lepidic pattern and invasive component ≤5 mm in their greatest dimension (12). To

date, imaging features have not been sufficiently described for MIAs; however, nonmucinous MIAs have been shown to appear as part-solid GGNs with a small solid component ≤5 mm (Fig. 3) or as pure GGNs (1, 11). Mucinous MIAs are much less frequent and may present as predominantly solid nodules (1).

Invasive adenocarcinomas with a predominant lepidic pattern can appear as part-solid GGNs with variable proportion of solid components (Fig. 4) (11). It is important to note that there is a significant imaging overlap between preinvasive lesions and invasive adenocarcinomas (13); both can appear as either pure or part-solid GGNs with only a difference in the frequency of each manifestation on a CT (13). The differentiation between the two entities based on imaging findings will be discussed in the following section.

Invasive mucinous adenocarcinoma, formerly referred to as mucinous BAC, is now recognized to have invasive components in a majority of the cases (12). The spectrum of imaging features for invasive mucinous adenocarcinoma varies widely from solid nodules or SSNs to lobar consolidations and may include air bronchograms or the CT angiogram sign (4, 11).

Further discrimination of subsolid nodules based on CT features

Given the poor prognosis of lung adenocarcinomas, it would be of the utmost importance to differentiate benign lesions from malignant tumors. Several studies have focused on the morphologic characteristics of SSNs for their differentiation. Lee et al. (14) reported that the predictive CT findings of malignancy were a size of >8 mm and a lobulated border for pure GGNs and a lobulated border for part-solid GGNs. Oda et al. (9) stated that an internal air bronchogram was more commonly associated with BAC than with AAH. In a different approach, Takahashi et al. (15) showed that a size of >10 mm, a lobulated margin and bubble-like appearance on initial CT were indicative of the future growth of pure GGNs, which implies probable malignancy.

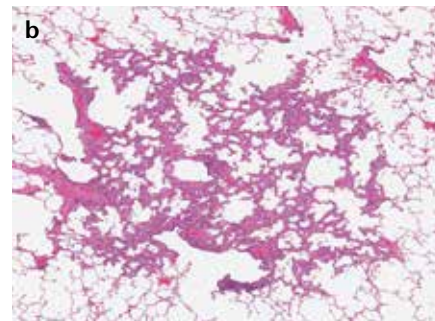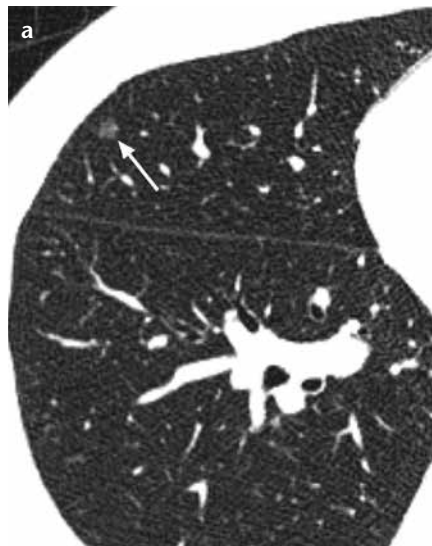Recently, Lee et al. (16) reported the differentiating CT features of invasive

Figure 1. a, b. Axial thin-section chest CT **(a)** and photomicrograph **(b)** (hematoxylin-eosin [H-E]; ×200) of an atypical adenomatous hyperplasia (AAH) in a 54-year old woman. AAH is usually a small, pure ground-glass nodule on CT *(arrow)* and is a proliferation of mildly to moderately atypical type II pneumocytes and/or Clara cells along the alveoli, pathologically.
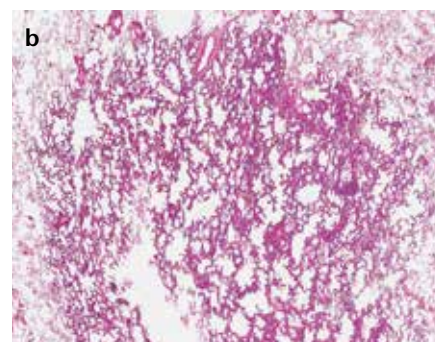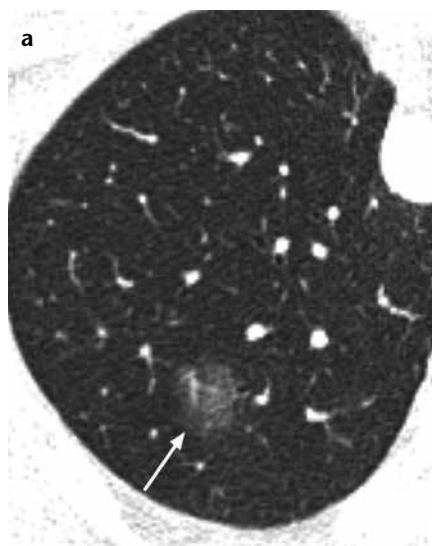

Figure 2. a, b. Axial thin-section chest CT **(a)** and photomicrograph **(b)** (H-E; ×100) of a nonmucinous adenocarcinoma *in situ* (AIS) in a 64-year old woman. AIS typically appears as a pure ground-glass nodule on CT *(arrow)* and is a small adenocarcinoma exhibiting lepidic growth without stromal, vascular, or pleural invasion, pathologically.

adenocarcinomas from preinvasive lesions (AAHs and AISs) appearing as SSNs in which preinvasive lesions can be candidates for limited resection or even close imaging follow ups. In pure GGNs, a lesion size of less than 10 mm specifically discriminated between preinvasive lesions and invasive adenocarcinomas (16). In part-solid GGNs, preinvasive lesions could accurately be distinguished from invasive adenocarcinomas by the smaller lesion size, smaller solid proportion, nonlobulated border, and nonspiculated margin (16). The mean nodule size and solid proportion of preinvasive lesions were 12.6±5.0 mm and 29.6±18.1%, respectively, while, for invasive lesions, they were 18.1±5.4 mm and 56.7±26.6%, respectively (16).

Importance of the solid component in subsolid nodules

The solid component of SSNs is known to represent the invasive foci of adenocarcinomas although other histologic changes, such as alveolar collapse, inflammation, fibrosis, and, occasionally, mucus, may appear as a solid region of SSNs on CT (4). The solid component is particularly important because it is related to the prognosis of the patient (17–19). Tsutani et al. (20) found that the size of the solid region was an independent predictor of nodal involvement in clinical stage IA lung adenocarcinomas. The size of the solid region was also found to be predictive of high-grade malignancy (positive lymphatic, vascular, or pleural invasion) and disease-free survival in clinical stage IA lung ad-

enocarcinomas (18). According to a study by Murakawa et al. (17), which included 241 patients with stage T1-2N0M0 lung adenocarcinomas, the ground-glass opacity (GGO) component showed little influence on tumor recurrence, and recurrence-free survival was solely dependent on the solid component size (17). In this context, the researchers even suggested that a T factor measured by the solid component might be a more accurate prognostic parameter (17).

Some studies revealed the importance of the proportion of the nodule that contained a solid component (21, 22). A prospective, multi-institutional study, which enrolled 811 patients with peripheral clinical IA lung cancer, showed that the tumor size ≤2.0 cm or ≤0.25 consolidation/tumor ratio at a lung window setting could be used as a radiologic criterion for noninvasive pathology, such as a tumor lacking nodal involvement, vascular invasion, or lymphatic invasion (22). In addition, patients who met the above criterion showed excellent survival after surgical resection and hilar/mediastinal lymph node dissection (97.1% for the five year overall and five year relapse-free survivals) (21). Similarly, the tumor disappearance rate (also known as the tumor vanishing ratio method), which is defined as the ratio between the GGN size measured at the lung window setting and at the mediastinal window setting, was suggested to have a prognostic value (23, 24).

Currently, the management plan for part-solid GGNs is determined by the size of the solid portion (2). Part-solid GGNs with solid components >5 mm should be considered malignant, and biopsy or surgical resection is recommended after confirmation of the persistence of the nodule (2). This recommendation is based on the new adenocarcinoma classification by the International Association for the Study of Lung Cancer, American Thoracic Society, and European Respiratory Society (IASLC/ATS/ERS) (12). Lesions in which the solid component measures 5 mm or less usually represent either AIS or MIA, in which case, conservative management may be indicated (2). The five-year disease-specific survival for both entities is nearly 100% if com-
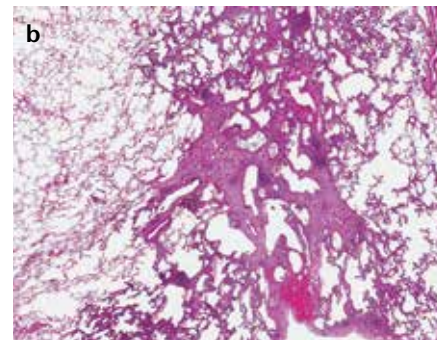
Figure 3. a, b. Axial thin-section chest CT **(a)** and photomicrograph **(b)** (H-E; ×100) of a nonmucinous minimally invasive adenocarcinoma (MIA) in a 76-year-old woman. MIA may appear as a part-solid ground-glass nodule (GGN) with a small solid component ≤5 mm or as a pure GGN on CT. This is a ≤3 cm lepidic predominant tumor and the largest dimension in the invasive area is ≤5 mm, pathologically.
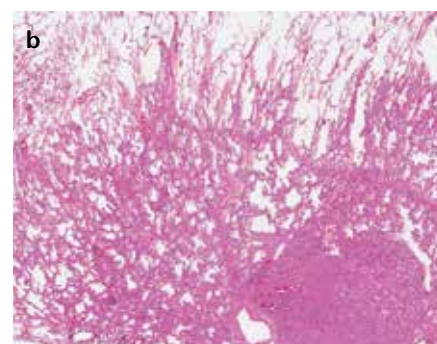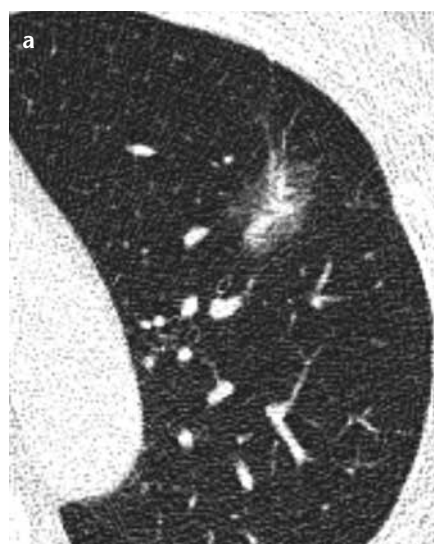
Figure 4. a, b. Axial thin-section chest CT **(a)** and photomicrograph **(b)** (H-E; ×100) of a lepidic predominant invasive adenocarcinoma in a 56-year-old man. This usually appears as a part-solid ground-glass nodule on CT and shows lepidic growth mostly with a >5 mm area of invasive adenocarcinoma, pathologically.

plete resection is achieved (2). These circumstances accentuate the importance of radiologic measurement of the solid component in part-solid GGNs. The new lung adenocarcinoma classification by IASLC/ATS/ERS recommends reporting both the solid component size as well as the total tumor size (12). The mediastinal window setting has frequently been used for identifying the solid portion (2); however, there is no standard criterion or definitive objective method for measuring the solid portion. Some researchers have used the lung window setting, instead of the mediastinal window setting, for the solid portion (19). The volumetric approach and Hounsfield unit (HU) threshold method are additional pos-

sible options for quantifying the solid portions.

Volumetric analysis of subsolid nodules

For small GGNs that lack a definite solid portion, differentiating malignant from benign GGNs is based on the detection of nodule growth on subsequent follow-up examinations. However, considering the slow growth of SSNs (25), early detection of growth on CT is not an easy task. SSN growth can manifest as an increase in the size and/or attenuation or the new occurrence of solid components within SSNs without a significant volume change (26). In this setting, computer-aided volumetry can be a helpful tool because it can provide accurate and

reproducible measurements (Fig. 5) (27). Several studies have reported promising SSN volumetry results (27), which we believe merit further studies with larger sample sizes.

Recently, de Hoop et al. (26) suggested a novel concept of using the mass measurement instead of the volume measurement for monitoring SSN growth. Mass is the integrative value of both the volume and attenuation and can reflect changes in both simultaneously. With manual volumetry using in-house software, de Hoop et al. (26) showed that mass measurements could detect the growth of SSNs earlier and that the mass was subject to less variability than the volume or diameter measurements. The mass measurement of SSNs using a commercial volumetric software program showed measurement variability ranging from -17.7% to 18.6%, and the largest measurement variability was attributable to the interscan variability (28). Recently, by comparing the CT attenuation values with histologic specimens, Zhang et al. (29) demonstrated that an increase of 100 HU in nodule attenuation represented an approximately 10% increase in tumor volume.

Role of FDG-PET for detecting subsolid nodules

Fluorine-18 fluorodeoxyglucose (^{18}F-FDG) positron emission tomography (PET) has been shown to accurately stage non-small cell lung cancers (NSCLCs) and, as a result, has been widely adopted as the standard for the evaluation of patients with NS-CLC (30). It has also been reported that glucose metabolism on ^{18}F-FDG PET correlates with the patient's prognosis (31–33). However, the role of ^{18}F-FDG PET for SSNs is not yet well established.

Kim et al. (30) reported a high false-negative rate of ^{18}F-FDG PET for identifying BACs. They stated that ^{18}F-FDG PET showed no clear advantage for the staging of lung cancer with predominant GGOs because of the low incidence of nodal and distant metastasis (30). Lee et al. (34) also insisted that ^{18}F-FDG PET should have only a limited role in the nodal staging of T1 SSNs because ^{18}F-FDG PET showed very low sensitivity and significantly lower accuracy than chest CT. In addition, no lymph node metastasis was present in patients with a solid proportion ≤50% according to Lee et al. (34) and Matsuguma et al. (35). In this context, ^{18}F-FDG PET is not recommended for the staging of small, pure GGNs.

Several researchers have suggested that ^{18}F-FDG PET could be helpful in the staging and prediction of the prognosis of stage IA adenocarcinomas (20, 36). Tsutani et al. (20) reported that the maximum standardized uptake values (SUV_{max}) was an independent predictor of nodal metastasis in clinical stage IA adenocarcinomas, and Okada et al. (36) showed that the SUV_{max} was a significant preoperative predictor for surgical outcomes including disease-free survival and overall survival. However, these studies dealt with both part-solid GGNs and solid tumors and did not focus on the prognostic role of ^{18}F-FDG PET in detecting SSNs. In spite of the Fleischner Society recommendation for PET imaging of part-solid nodules larger than 10 mm (Fig. 6) (2), the usefulness of ^{18}F-FDG PET for SSNs remains in question. Conclusions regarding this issue should be deferred until future prospective studies provide us with more data.

Natural clinical course of subsolid nodules

With respect to screening-detected SSNs, it has been reported that 37% to 70% of nodules are transient and disappear on follow-up studies (1). Transient SSNs are associated with infectious or inflammatory conditions, and blood eosinophilia is one of the well-known causes of transient inflammation in the lung (1, 37). Lee et al. (37) reported that transient SSNs are related to features such as a young patient age, detection at follow up, blood eosinophilia, lesion multiplicity, a large solid portion, and an ill-defined lesion border.

Persistent SSNs are generally known to grow slowly; however, the exact natural history of SSNs has not been extensively investigated to date (Table 1). Some retrospective studies have revealed that part-solid GGNs grow faster than pure GGNs and that adenocarcinomas manifesting as SSNs showed shorter volume doubling

Figure 5. a–c. Volumetric analysis of a 13 mm part-solid ground-glass nodule **(a)** in a 54-year-old female using a commercial software package (LungCARE, Siemens Healthcare, Erlangen, Germany). After determining the volume of interest *(yellow square)* on thin-slab, maximum intensity projection images **(b)**, a volume-rendered image of a nodule and the surrounding structures **(c)** is obtained with simultaneous calculation of the nodule volume and attenuation.
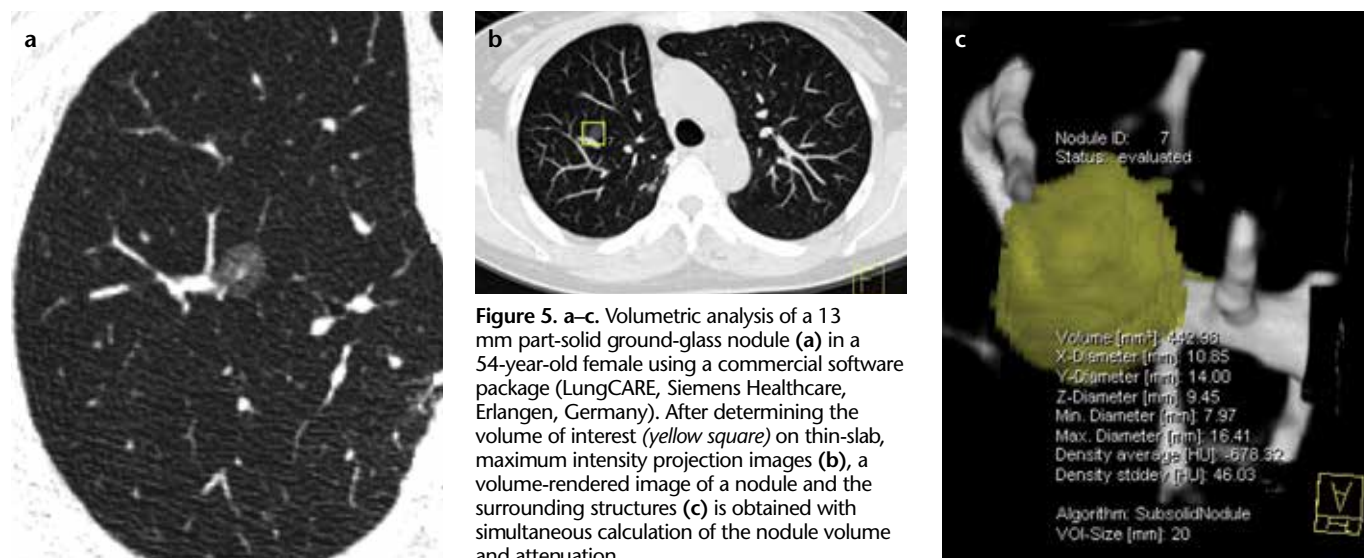
Table 1. Publications on the natural history of pulmonary subsolid nodules and their growth rate

First author	Year published	Study design	Follow-up period	Inclusion of patients with past for pure malignancy	Growing proportion for pure GGNs (n, %)	Growing proportion for part-solid GGNs (n, %)	VDT for overall, pure, or for part-solid GGNs, if recorded (days)[a]
Aoki et al. (63)	2000	Retrospective	N/A	N/A	N/A	N/A	Overall, 880 (range, 662–1486)[b]
Hasegawa et al. (38)	2000	Retrospective	Mean, 458 days	N/A	N/A	N/A	Pure, 813±375[c] Part-solid, 457±260[c]
Kodama et al. (43)	2002	Retrospective	Median, 32 months	Yes	11/19 (58)	N/A	N/A
Kakinuma et al.[d] (64)	2004	Retrospective	Mean, 17 months	N/A	N/A	N/A	Pure, 417±220 (range, 198–669)[e]
Lindell et al.[f] (65)	2007	Retrospective	N/A	No	N/A	N/A	Pure, 469±452[c] Part-solid, 568±1222[c]
Hiramatsu et al. (42)	2008	Retrospective	Median, 1048 days	Yes	14/95 (15)	12/30 (40)	N/A
Saito et al. (66)	2009	Retrospective	Median, 732 days	N/A	N/A	N/A	Overall, 770±914 (range, 225–1402)[g]
Oda et al.[h] (39)	2011	Retrospective	Mean, 188 days	N/A	N/A	N/A	Overall, 486±369 (range, 89–1583)[i] Pure, 629±404 (range, 154–1583)[i] Part-solid, 277±156 (range, 89–725)[i]
Silva et al.[j] (41)	2012	Prospective	Mean, 50 months	No	8/48 (17)	12/26 (46)[k]	N/A
Takahashi et al.[l] (15)	2012	Retrospective	Mean, 66 months	Yes	19/150 (13)	N/A	Pure, 1248±600 (range, 360–2439)
Chang et al. (40)	2013	Retrospective	Mean, 59 months	No	12/122 (10)	N/A	Pure, median, 769 (range, 330–3031)
Kobayashi et al. (44)	2013	Retrospective	Mean, 4.2 years	Yes	29/108 (27)[m]	N/A	N/A
Matsuguma et al. (67)	2013	Retrospective	Mean, 29 months	Yes	14/98 (14)[n]	27/76 (36)[n]	N/A

[a]Unless otherwise specified, data are given as mean±standard deviation.
[b]VDT for ≤3 cm Noguchi type A and B lesions, which included five tumors with >50% of GGO proportion and one solid nodule. The VDT was calculated using the mean of the longest and shortest diameters of the tumor measured on the initial and final chest radiography.
[c]Volume was calculated using bidimensional measurements of the maximum and perpendicular diameters.
[d]This study included histologically diagnosed pure GGNs >5 mm at initial thin-section CT.
[e]The VDT was calculated using the means of the length and width of the lesion.
[f]The study population was extracted from a prospective study in which screening CT scans were obtained initially and every 12 months thereafter for five years.
[g]Noguchi type A, B, C, and D lesions were included and described as "GGO-like lesions".
[h]Histologically diagnosed subsolid nodules ≤30 mm were included.
[i]Calculation of the VDT was based on computer-aided three-dimensional volumetry (3D-analysis software, Fujitsu, Tokyo, Japan).
[j]The study population was extracted from the Multicentric Italian Lung Detection (MILD) trial at the National Cancer Institute of Milan.
[k]Data are for part-solid GGNs with a solid component smaller than 5 mm.
[l]This study included pure GGNs ≤15 mm at initial detection.
[m]This study did not report the growing proportion of pure and part-solid GGNs separately. Among 108 subsolid nodules with 82 pure and 26 part-solid GGNs, 29 showed interval growth.
[n]This study included subsolid nodules ≤2 cm in diameter and >20% in GGO portion. The estimated two-year and five-year cumulative percentages of growing nodules were 13% and 23% for nonsolid nodules and 38% and 55% for part-solid nodules, respectively.
GGN, ground-glass nodule; GGO, ground-glass opacity; N/A, not applicable; VDT, volume doubling time.
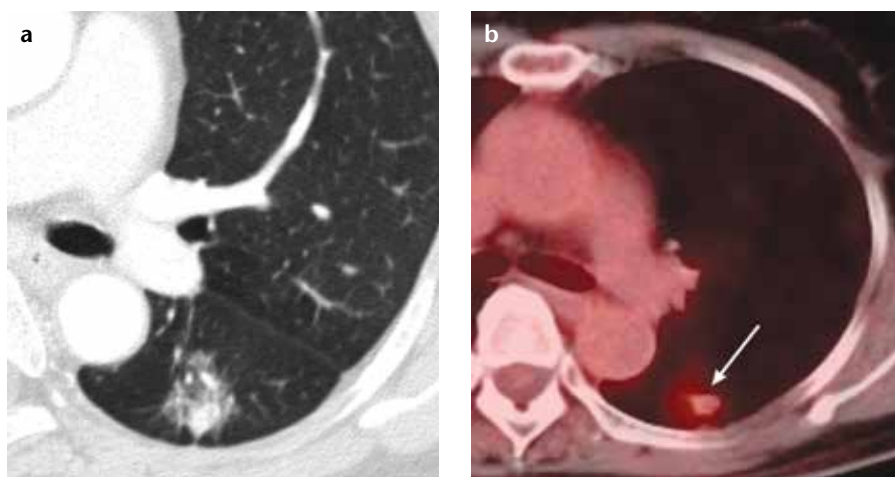
Figure 6. a, b. A case of an invasive adenocarcinoma in a 63-year-old female, which appeared as a part-solid ground-glass nodule on CT **(a)**. On ^{18}F-FDG PET **(b)**, this nodule *(arrow)* showed an increased maximum standardized uptake value of 2.7.

times (VDTs) than preinvasive lesions (38, 39). According to Oda et al. (39), the mean VDTs for AAHs, BACs, and adenocarcinomas were 859.2±428.9, 421.2±228.4, and 202.1±84.3 days, respectively. The mean VDTs for pure and part-solid GGNs were 628.5±404.2 and 276.9±155.9 days, respectively (39). Interestingly, the VDTs of part-solid GGNs that were proven to be adenocarcinomas were shorter than those of pure-GGNs that were also histologically proven to be adenocarcinomas (457±260 vs. 813±375 days) (39). With the finding that the internal attenuation of SSNs had a significant correlation with the VDT, Oda et al. (39) suggested that SSNs with high

internal attenuation require more careful observation.

Recently, researchers have focused on screening-detected SSNs, which have been one of the main interests of radiologists. Regarding screening-detected pure GGNs in patients who lack a past history of malignancy, growth was observed in 9.8%–16.7% after a mean or median follow-up period of 50–59 months (40, 41). Thus, the majority of pure GGNs remained stable on later follow-up. On the other hand, in study populations, which included patients with a history of malignancy, a much higher proportion (15%–58%) of pure GGNs showed interval growth (42, 43). These studies indicate that a history of past malignancy is a risk factor for nodule growth. In addition, Chang et al. (40) found that the initial size and the development of a new solid portion were significantly associated with nodule growth in patients with pure GGNs.

For part-solid GGNs, growth was observed in 40%–46.2% after a mean or median follow-up period of 35–59 months (41, 42). In a study population from the Multicentric Italian Lung Detection (MILD) project, Silva et al. (41) disclosed the natural course of part-solid GGNs with a solid component smaller than 5 mm. Among the 26 part-solid GGNs, 12 (46.2%) progressed, 11 (42.3%) remained stable, and three (11.5%) resolved (41). These findings were meaningful given that approximately half of the part-solid GGNs currently indicated to undergo surveillance would eventually show growth.

Considering the indolent growth and the small number of SSNs that show interval growth during follow-up, long-term follow-up is essential in the management of SSNs, particularly pure GGNs. Kobayashi et al. (44) suggested that SSNs should be monitored for at least three years, based on their finding that all growing SSNs showed growth within three years of their first observation. Silva et al. (41) reported that one of the pure GGNs in their study developed a new solid component after 63.9 months. Chang et al. (40) insisted that the follow-up duration of SSNs should be extended to five or ten years.

Imaging-guided biopsy of subsolid nodules

With respect to the biopsy of SSNs, several CT-based approaches including sequential CT-guided-biopsy, CT fluoroscopy-guided biopsy, and cone-beam CT (CBCT) virtual-navigation-guided biopsy have been introduced (45–49). Either a fine needle aspiration biopsy or a core biopsy can be used, but core biopsy showed higher diagnostic accuracy (46, 49). The reported diagnostic accuracy of CT-based biopsy for SSNs ranged from 64.6% to 93.0% (45–49).

Regarding CT fluoroscopy-guided needle aspiration biopsy, Hur et al. (45) reported a diagnostic sensitivity, specificity, and accuracy of 71%, 100%, and 82%, respectively. CT fluoroscopy-guided core biopsy showed a higher diagnostic accuracy of 90.6% in a more recent study (49). Notably, the diagnostic accuracy of CT fluoroscopy-guided needle aspiration or core biopsy for pure GGNs was lower than that for part-solid GGNs (45, 49), which would be due to the low cellularity of pure GGNs (45). However, Kim et al. (46), using CT-guided core biopsy, reported conflicting results that the diagnostic accuracy was not influenced by the proportion of the GGO component. We do not currently have a definite conclusion on whether biopsy would provide accurate diagnosis for SSNs.

Recently, Lu et al. (47) revealed that stromal invasion was underestimated in 43.5% of CT-guided core biopsy specimens, especially in pure GGNs, compared to the surgical pathology. Kim et al. (46) also reported an underestimation of the pathologic grade on biopsy. Among the 13 patients initially diagnosed as having BAC at the core biopsy in the study by Kim et al. (46), seven patients were confirmed to have adenocarcinomas with a BAC feature.

According to Choo et al. (50), CBCT virtual-navigation-guided biopsy showed an excellent diagnostic yield for small (≤1 cm) lung nodules with a sensitivity, specificity, and accuracy of 96.7%, 100%, and 98.0%. Approximately 10% of the nodules were SSNs in the Choo et al. study (50). CBCT-guided biopsy is expected to show high diagnostic accuracy for SSNs (Fig. 7); however, the diagnostic performance of CBCT-guided biopsy for SSNs requires further validation with a larger study population.

Considering the findings that CT-based biopsy might not provide a satisfactory diagnostic yield for small pure GGNs and that small invasive foci could not be accurately sampled, CT-based biopsy alone may have some limitations for the pathologic confirmation of SSNs. In addition, postbiopsy hemoptysis was found to be more common in SSNs than in solid tumors (51). Thus, if the suspicion for malignancy in a SSN is high on CT (e.g., persistent part-solid nodule) or if there is any increase in the size of the whole lesion or solid portion of SSNs, CT-guided biopsy may be bypassed, and surgical biopsy can be performed to obtain a pathologic diagnosis (13, 52).

Localization of subsolid nodules prior to surgery

In addition to biopsy, there is another important radiologic interventional procedure for SSNs. Because SSNs are often impalpable in the operation field and indistinguishable from the normal parenchyma exteriorly, preoperative marking techniques have been reported for localization during thoracoscopic surgery using a dye, colored collagen, barium, lipiodol, microcoil, or a metallic wire (53). Either a percutaneous approach or a transbronchial approach can be used (54).

Today, metallic hook wire localization under CT guidance is the most widely used technique (54). CT-guided hook wire localization is accurate in localizing the lesion, is simple to operate, and helps facilitate the complete excision of the nodule by the use of an endostapler because the presence of a wire hook makes it possible to exert slight traction (55). However, wire dislodgement occurs in up to 20% of these cases, and having a metallic wire in the chest wall can be uncomfortable for the patients (54).

Lee et al. (54) recently reported their results on CT-guided percutaneous barium marking of SSNs prior to video-assisted thoracoscopic surgery (VATS) (Fig. 8). In their study, all target nodules were marked within a 3 mm distance from the injected barium sulfate suspension, and all barium balls were
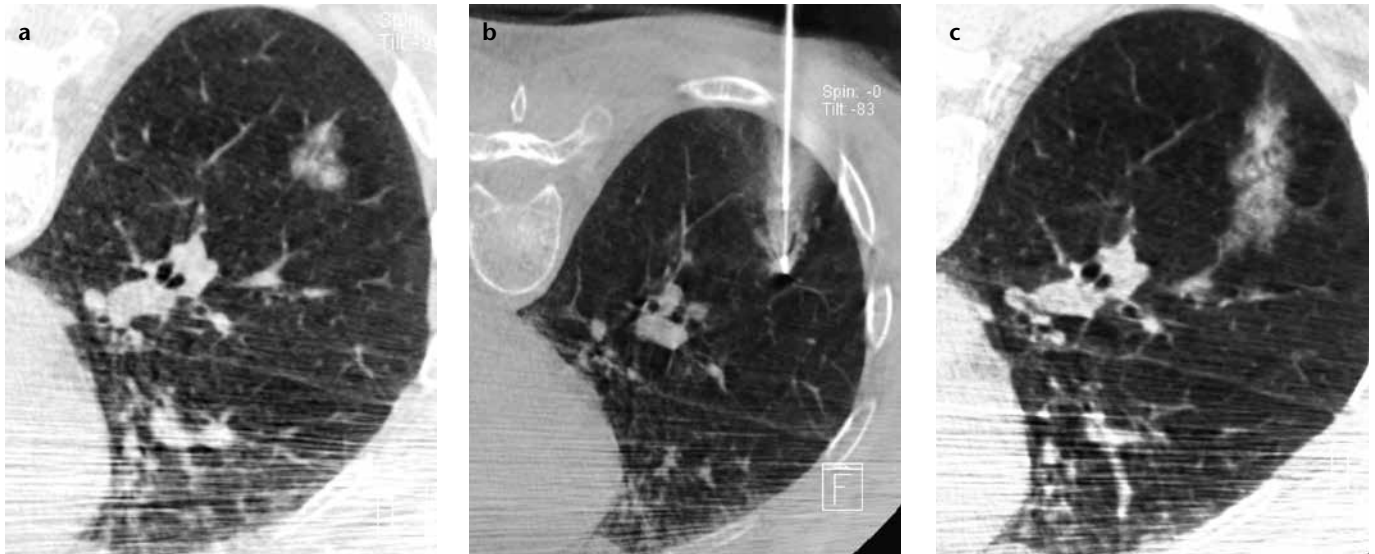
Figure 7. a–c. Cone-beam CT-guided core biopsy of a part-solid ground-glass nodule in the right lower lobe of the lung taken in the prone position **(a, b)**. Note the hemorrhage along the needle insertion pathway on the postbiopsy cone-beam CT **(c)**. The loose compactness of subsolid nodules might increase the risk of hemoptysis after cutting needle biopsy.
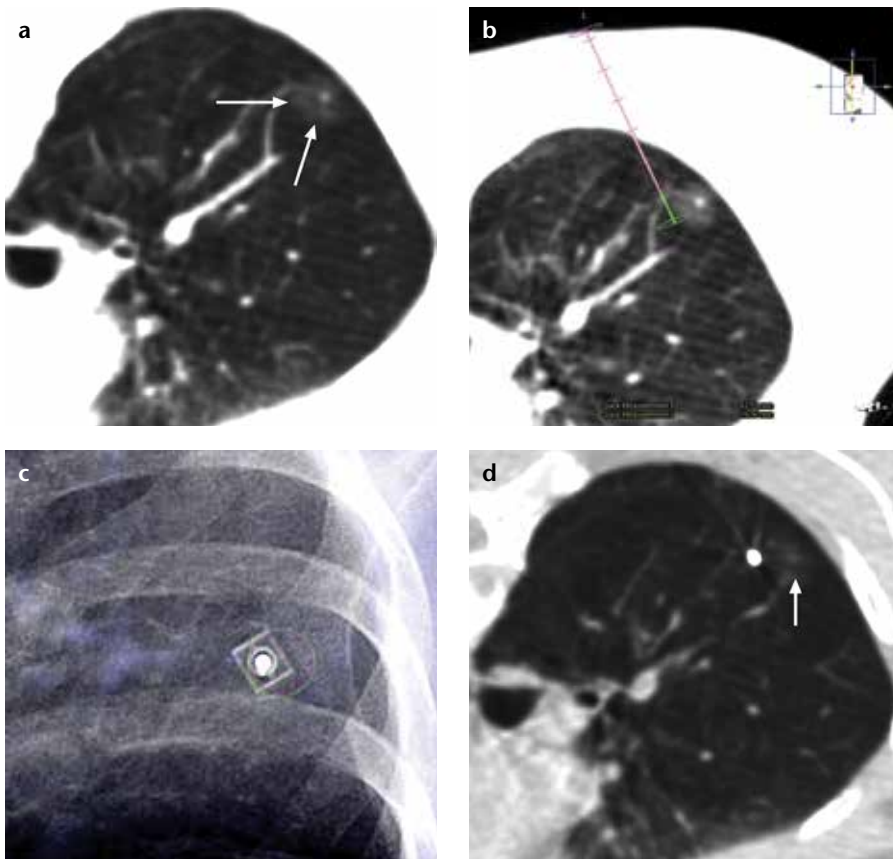

Figure 8. a–d. CT-guided percutaneous barium marking of a part-solid ground-glass nodule in a 54-year-old female prior to video-assisted thoracoscopic surgery. After obtaining a preprocedural cone-beam CT scan of the nodule **(a,** *arrows)*, the entry site, intended barium injection focus, and needle route were determined **(b)**. A needle was introduced in the bull's eye view **(c)**, and injection of barium sulfate suspension was successfully performed **(d)** beside the nodule *(arrow)*. Direct barium injection into the nodule should be avoided because barium-related acute inflammation may interfere with the pathologic diagnosis.

completely resected after visualization by intraoperative fluoroscopy (54).

One advantage of this technique is the flexible scheduling of time in the op-

eration room because barium remains in the body for a relatively long period of time (56). Care should be taken to avoid directly injecting the barium into the target nodule, which could otherwise interfere with the pathologic diagnosis of the target nodule due to acute inflammation associated with barium materials (54). In this respect, lipiodol should be considered as an alternative because lipiodol is known to induce only minimal inflammation in a few hours (57).

Several researchers have suggested that CT-guided radioactive dye injection, which uses microspheres of human albumin serum labeled with Technetium-99m (99mTc), is preferable to subcentimeter nodules during VATS because it offers higher sensitivity, minimal operator dependence, minimal complications and a lower risk of failures (58). However, this novel method requires preparation of 99mTc-labeled albumin prior to the procedure and requires a special probe during surgery to convert radioactivity into an audio signal.

Surgical approach for subsolid nodules

Lobectomy with lymph node dissection has been the standard for lung cancer resection. However, many Japanese investigators have suggested limited resection including wedge resection without lymph node dissection or

Table 2. Management guidelines for pulmonary subsolid nodules recommended by Fleischner Society (2)

Nodule type	Recommendations
Initial detection	
Pure GGN(s) ≤5 mm	No CT follow-up required for a solitary lesion
	If multiple, CT follow-up at two and four years
Pure GGN(s) >5 mm and part-solid GGN(s) of any size	Initial follow-up CT at three months to confirm the lesions' persistence
Solitary persistent nodule	
Pure GGN >5 mm	Annual surveillance CT for at least three years if persistent at three months follow-up CT
Part-solid GGN with solid component ≤5 mm	Annual surveillance CT for at least three years if persistent at three months follow-up CT
Part-solid GGN with solid component >5 mm	Biopsy or surgical resection if persistent
Multiple persistent nodules	
Pure GGNs >5 mm	Annual surveillance CT for at least three years
Dominant nodule with part-solid or solid component	Dominant lesion determines further management
	Biopsy or resection for part-solid with solid component >5 mm

CT, computed tomography; GGN, ground-glass nodule.

segmentectomy based on the excellent prognosis and very low probability of lymph node metastasis of peripheral small adenocarcinomas appearing as SSNs (59, 60). A few studies have reported good survival after limited resection of peripheral early stage lung cancers, and some have even stated that long-term survival after limited resection was equivalent to that after lobectomy (21, 61). In addition, limited resection preserved more lung function postoperatively than did lobectomy (62). This is important in that limited resection would offer patients a higher tolerance for the second lung resection, given that as many as 11.5% of patients who undergo resection of lung cancer develop additional primary lung cancers within their lifetimes (60). However, it is difficult to draw definite conclusions from the above studies because these were not randomized trials and involved relatively short follow-up intervals. In fact, according to one prospective study that reported a long-term outcome after a median follow-up period of 10 years, limited resection (wedge or segment) of clinical T1N0M0 SSNs showed a low disease-control rate of 85% (59). Of 26 patients, adenocarcinomas developed in four in the area surrounding the initial limited resection site after more than five years (59).

The role of limited resection may be clarified by currently ongoing randomized controlled clinical trials. A single-arm, limited-resection trial referred to as the Japanese Clinical Oncology Group (JCOG) 0804/West Japan Oncology Group (WJOG) 4507L, is in progress for subsolid T1aN0M0 peripheral tumors with a consolidation-tumor size ratio of 0.25 or less. Two other phase III randomized trials of standard lobectomy versus experimental limited resection for small (≤2 cm in diameter) peripheral non-small cell lung cancers are also ongoing in the United States (CALGB-140503) and in Japan (JCOG0802/WJOG4607L). These trials will hopefully provide compelling evidence for the selection of the surgical extent of SSNs.

Current management guidelines from the Fleischner Society

Recently, the Fleischner Society published recommendations for the management of SSNs (2). The recommendations include guidelines for single pure and part-solid GGNs as well as for multiple GGNs with or without a dominant nodule. Guidelines are specified according to the size of the nodule and solid portion and are written with special consideration for SSNs confirmed to persist after initial follow-up CT at three months (2). One notable point is the consideration of the new adenocarcinoma classification (12). As mentioned above, patients with AIS or MIA who undergo complete surgical resection should have 100% or near 100% five-year disease-free survival (2). Thus,

solitary part-solid nodules with solid portion sizes ≤5 mm may be conservatively monitored without immediate resection or biopsy (2).

An important prerequisite for the Fleischner Society guidelines is adequate acquisition and interpretation of a chest CT (2). First, thin-section CT is required, ideally with 1 mm section thickness. Second, the GGO component is evaluated with the lung window setting, whereas the solid component is evaluated on the mediastinal window setting. Third, bidimensional measurements should be acquired with an electronic caliper. The recommendations are based on the average of the long and short dimensions and the same measurement method should be consistently applied to all subsequent CT acquisitions. Last but not least, each examination should be compared to the initial imaging findings to detect the subtle growth of SSNs.

In addition, there are several issues worth noting. It is important to recognize that not all lesions with slight size decreases are necessarily benign, particularly when they are associated with an increase in attenuation because adenocarcinomas can decrease temporarily in size owing to fibrosis or atelectasis (2). SSNs that enlarge and/or increase in attenuation with or without the new appearance of a solid component during follow up should be managed with a high degree of suspicion and an aggressive approach is

recommended. Furthermore, risk factors such as smoking history, familial history of lung cancer or exposure to carcinogenic agents are not considered in the current guidelines due to a lack of sufficient data (2).

Detailed recommendations are as follows (Table 2) (2):

1) Solitary, pure GGNs measuring 5 mm or less do not require follow-up surveillance CT examinations.

2) Solitary, pure GGNs larger than 5 mm require an initial follow-up CT examination within three months, to determine persistence, followed by yearly surveillance CT examinations for a minimum of three years if they are persistent and unchanged. ^{18}F-FDG PET is of low value due to its high false negative rate and biopsy is not routinely recommended. For lesions that enlarge and/or increase in attenuation, surgical resection should be considered.

3) Solitary part-solid GGNs, especially those in which the solid component is larger than 5 mm, should be considered malignant until proven otherwise, provided either growth or no change is observed during the follow-up CT examination performed at three months. For part-solid GGNs of 8–10 mm, further evaluation with ^{18}F-FDG PET is advisable and biopsy is not routinely recommended unless surgery is not an option. Part-solid GGNs with a solid portion ≤5 mm may be followed-up with yearly surveillance CT for a minimum of three years.

4) Multiple, well-defined GGNs all measuring 5 mm or less should be conservatively managed with follow-up CT examinations performed at two and four years.

5) In cases in which multiple pure GGNs are identified, at least one of which is larger than 5 mm, and in the absence of a dominant lesion, an initial follow-up CT examination at three months is recommended, followed by long-term yearly surveillance CT examinations for at least three years. Routine use of ^{18}F-FDG PET or biopsy is not recommended. Dominant lesions refer to part-solid GGNs with solid components larger than 5 mm; pure GGNs larger than 10 mm; atypical subsolid nodules with spiculated contours, bubbly appearance or reticulation; pure GGNs or part-solid GGNs with solid components smaller than 5 mm that demonstrate an interval change in size or attenuation or solid lesions with characteristics suspicious of invasive carcinoma.

6) In cases with multiple subsolid nodules in which a dominant lesion(s) can be identified, the dominant lesion(s) is used to determine further management. After an initial follow-up CT examination at three months that confirms persistence, an aggressive approach to diagnosis and management is recommended, especially for lesions with solid components larger than 5 mm. For part-solid GGNs of 8–10 mm, further evaluation with ^{18}F-FDG PET is advisable.

Conclusion

Subsolid nodules, particularly when they persist throughout follow up, represent a spectrum of diseases from AAH to invasive adenocarcinoma. AAHs usually appear as small pure GGNs, whereas AISs, MIAs, and invasive adenocarcinomas can appear as either pure or part-solid GGNs. For differentiating between preinvasive and invasive lesions, several morphologic characteristics, such as a larger nodule size, a greater solid proportion, a lobulated border, or a spiculated margin, have been suggested. However, these findings have not yet proven sufficiently reliable to guide the management plan. In addition, given that the solid component in GGNs is related to the invasiveness of the tumor as well as the patient's prognosis, evaluation and follow-up of the solid portion is particularly important. SSNs are generally known to grow slowly; thus, long-term follow-up for at least three years is essential. With respect to radiologic intervention, CT-based nodule localization prior to surgery is a useful procedure in the management of SSNs. Lastly, recent Fleischner Society recommendations for SSNs should help radiologists with the follow-up of nodules in clinical practice.

Conflict of interest disclosure

The authors declared no conflicts of interest.

References

1. Godoy MCB, Naidich DP. Overview and strategic management of subsolid pulmonary nodules. J Thoracic Imaging 2012; 27:240–248. [CrossRef]

2. Naidich DP, Bankier AA, MacMahon H, et al. Recommendations for the management of subsolid pulmonary nodules detected at CT: a statement from the Fleischner society. Radiology 2013; 266:304–317. [CrossRef]

3. Henschke CI, Yankelevitz DF, Mirtcheva R, et al. CT screening for lung cancer: frequency and significance of part-solid and nonsolid nodules. Am J Roentgenol 2002; 178:1053–1057. [CrossRef]

4. Austin JHM, Garg K, Aberle D, et al. Radiologic implications of the 2011 classification of adenocarcinoma of the lung. Radiology 2013; 266:62–71. [CrossRef]

5. Park CM, Goo JM, Lee HJ, Lee CH, Chun EJ, Im JG. Nodular ground-glass opacity at thin-section CT: histologic correlation and evaluation of change at follow-up. Radiographics 2007; 27:391–408. [CrossRef]

6. Park CM, Goo JM, Lee HJ, et al. Focal interstitial fibrosis manifesting as nodular ground-glass opacity: thin-section CT findings. Eur Radiol 2007; 17:2325–2331. [CrossRef]

7. Jang HJ, Lee KS, Kwon OJ, Rhee CH, Shim YM, Han J. Bronchioloalveolar carcinoma: focal area of ground-glass attenuation at thin-section CT as an early sign. Radiology 1996; 199:485–488.

8. Mori M, Rao SK, Popper HH, Cagle PT, Fraire AE. Atypical adenomatous hyperplasia of the lung: a probable forerunner in the development of adenocarcinoma of the lung. Modern Pathol 2001; 14:72–84. [CrossRef]

9. Oda S, Awai K, Liu D, et al. Ground-glass opacities on thin-section helical CT: differentiation between bronchioloalveolar carcinoma and atypical adenomatous hyperplasia. Am J Roentgenol 2008; 190:1363–1368. [CrossRef]

10. Park CM, Goo JM, Lee HJ, et al. CT findings of atypical adenomatous hyperplasia in the lung. Korean J Radiol 2006; 7:80–86. [CrossRef]

11. Lee HJ, Lee CH, Jeong YJ, et al. IASLC/ATS/ERS international multidisciplinary classification of lung adenocarcinoma: novel concepts and radiologic implications. J Thorac Imaging 2012; 27:340–353. [CrossRef]

12. Travis WD, Brambilla E, Noguchi M, et al. International association for the study of lung cancer/american thoracic society/european respiratory society international multidisciplinary classification of lung adenocarcinoma. J Thorac Oncol 2011; 6:244–285. [CrossRef]

13. Goo JM, Park CM, Lee HJ. Ground-glass nodules on chest CT as imaging biomarkers in the management of lung adenocarcinoma. Am J Roentgenol 2011; 196:533–543. [CrossRef]

14. Lee HJ, Goo JM, Lee CH, et al. Predictive CT findings of malignancy in ground-glass nodules on thin-section chest CT: the effects on radiologist performance. Eur Radiol 2009; 19:552–560. [CrossRef]

15. Takahashi S, Tanaka N, Okimoto T, et al. Long term follow-up for small pure ground-glass nodules: implications of determining an optimum follow-up period and high-resolution CT findings to predict the growth of nodules. Jpn J Radiol 2012; 30:206–217. [CrossRef]

16. Lee SM, Park CM, Goo JM, Lee HJ, Wi JY, Kang CH. Invasive pulmonary adenocarcinomas versus preinvasive lesions appearing as ground-glass nodules: differentiation by using CT features. Radiology 2013; 268:265–273. [CrossRef]

17. Murakawa T, Konoeda C, Ito T, et al. The ground glass opacity component can be eliminated from the T-factor assessment of lung adenocarcinoma. Eur J Cardiothorac Surg 2013; 43:925–932. [CrossRef]

18. Tsutani Y, Miyata Y, Nakayama H, et al. Prognostic significance of using solid versus whole tumor size on high-resolution computed tomography for predicting pathologic malignant grade of tumors in clinical stage IA lung adenocarcinoma: a multicenter study. J Thorac Cardiovasc Surg 2012; 143:607–612. [CrossRef]

19. Tsutani Y, Miyata Y, Yamanaka T, et al. Solid tumors versus mixed tumors with a ground-glass opacity component in patients with clinical stage IA lung adenocarcinoma: Prognostic comparison using high-resolution computed tomography findings. J Thorac Cardiovasc Surg 2013; 146:17–23. [CrossRef]

20. Tsutani Y, Miyata Y, Nakayama H, et al. Prediction of pathologic node-negative clinical stage IA lung adenocarcinoma for optimal candidates undergoing sublobar resection. J Thorac Cardiovasc Surg 2012; 144:1365–1371. [CrossRef]

21. Asamura H, Hishida T, Suzuki K, et al. Radiographically determined noninvasive adenocarcinoma of the lung: survival outcomes of Japan Clinical Oncology Group 0201. J Thorac Cardiovasc Surg 2013; 146:24–30. [CrossRef]

22. Suzuki K, Koike T, Asakawa T, et al. A prospective radiological study of thin-section computed tomography to predict pathological noninvasiveness in peripheral clinical IA lung cancer (Japan Clinical Oncology Group 0201). J Thorac Oncol 2011; 6:751–756. [CrossRef]

23. Haraguchi N, Satoh H, Kikuchi N, Kagohashi K, Ishikawa H, Ohtsuka M. Prognostic value of tumor disappearance rate on computed tomography in advanced-stage lung adenocarcinoma. Clin Lung Cancer 2007; 8:327–330. [CrossRef]

24. Kakinuma R, Kodama K, Yamada K, et al. Performance evaluation of 4 measuring methods of ground-glass opacities for predicting the 5-year relapse-free survival of patients with peripheral nonsmall cell lung cancer: a multicenter study. J Comput Assist Tomogr 2008; 32:792–798. [CrossRef]

25. Godoy MCB, Naidich DP. Subsolid pulmonary nodules and the spectrum of peripheral adenocarcinomas of the lung: recommended interim guidelines for assessment and management. Radiology 2009; 253:606–622. [CrossRef]

26. de Hoop B, Gietema H, van de Vorst S, Murphy K, van Klaveren RJ, Prokop M. Pulmonary ground-glass nodules: increase in mass as an early indicator of growth. Radiology 2010; 255:199–206. [CrossRef]

27. Goo JM. A computer-aided diagnosis for evaluating lung nodules on chest CT: the current status and perspective. Korean J Radiol 2011; 12:145–155. [CrossRef]

28. Kim H, Park CM, Woo S, et al. Pure and part-solid pulmonary ground-glass nodules: measurement variability of volume and mass in nodules with a solid portion less than or equal to 5 mm. Radiology. 2013 Jul 17. [Epub ahead of print] [CrossRef]

29. Zhang LJ, Yankelevitz DF, Carter D, Henschke CI, Yip R, Reeves AP. Internal growth of nonsolid lung nodules: radiologic-pathologic correlation. Radiology 2012; 263:279–286. [CrossRef]

30. Kim TJ, Park CM, Goo JM, Lee KW. Is there a role for FDG PET in the management of lung cancer manifesting predominantly as ground-glass opacity? Am J Roentgenol 2012; 198:83–88. [CrossRef]

31. Erasmus JJ, Rohren E, Swisher SG. Prognosis and reevaluation of lung cancer by positron emission tomography imaging. Proc Am Thorac Soc 2009; 6:171–179. [CrossRef]

32. Um SW, Kim H, Koh WJ, et al. Prognostic value of F-18-FDG uptake on positron emission tomography in patients with pathologic stage I non-small cell lung cancer. J Thorac Oncol 2009; 4:1331–1336. [CrossRef]

33. Weber WA, Petersen V, Schmidt B, et al. Positron emission tomography in non-small-cell lung cancer: prediction of response to chemotherapy by quantitative assessment of glucose use. J Clin Oncol 2003; 21:2651–2657. [CrossRef]

34. Lee SM, Park CM, Paeng JC, et al. Accuracy and predictive features of FDG-PET/CT and CT for diagnosis of lymph node metastasis of T1 non-small-cell lung cancer manifesting as a subsolid nodule. Eur Radiol 2012; 22:1556–1563. [CrossRef]

35. Matsuguma H, Yokoi K, Anraku M, et al. Proportion of ground-glass opacity on high-resolution computed tomography in clinical T1 N0 M0 adenocarcinoma of the lung: a predictor of lymph node metastasis. J Thorac Cardiovasc Surg 2002; 124:278–284. [CrossRef]

36. Okada M, Nakayama H, Okumura S, et al. Multicenter analysis of high-resolution computed tomography and positron emission tomography/computed tomography findings to choose therapeutic strategies for clinical stage IA lung adenocarcinoma. J Thorac Cardiovasc Surg 2011; 141:1384–1391. [CrossRef]

37. Lee SM, Park CM, Goo JM, et al. Transient part-solid nodules detected at screening thin-section CT for lung cancer: comparison with persistent part-solid nodules. Radiology 2010; 255:242–251. [CrossRef]

38. Hasegawa M, Sone S, Takashima S, et al. Growth rate of small lung cancers detected on mass CT screening. Br J Radiol 2000; 73:1252–1259.

39. Oda S, Awai K, Murao K, et al. Volume-doubling time of pulmonary nodules with ground glass opacity at multidetector CT: assessment with computer-aided three-dimensional volumetry. Acad Radiol 2011; 18:63–69. [CrossRef]

40. Chang B, Hwang JH, Choi YH, et al. Natural history of pure ground-glass opacity lung nodules detected by low-dose CT scan. Chest 2013; 143:172–178. [CrossRef]

41. Silva M, Sverzellati N, Manna C, et al. Long-term surveillance of ground-glass nodules: evidence from the MILD trial. J Thorac Oncol 2012; 7:1541–1546. [CrossRef]

42. Hiramatsu M, Inagaki T, Inagaki T, et al. Pulmonary ground-glass opacity (GGO) lesions-large size and a history of lung cancer are risk factors for growth. J Thorac Oncol 2008; 3:1245–1250. [CrossRef]

43. Kodama K, Higashiyama M, Yokouchi H, et al. Natural history of pure ground-glass opacity after long-term follow-up of more than 2 years. Ann Thorac Surg 2002; 73:386–92. [CrossRef]

44. Kobayashi Y, Fukui T, Ito S, et al. How long should small lung lesions of ground-glass opacity be followed? J Thorac Oncol 2013; 8:309–314.

45. Hur J, Lee HJ, Nam JE, et al. Diagnostic accuracy of CT fluoroscopy-guided needle aspiration biopsy of ground-glass opacity pulmonary lesions. Am J Roentgenol 2009; 192:629–634. [CrossRef]

46. Kim TJ, Lee JH, Lee CT, et al. Diagnostic accuracy of CT-guided core biopsy of ground-glass opacity pulmonary lesions. Am J Roentgenol 2008; 190:234–239. [CrossRef]

47. Lu CH, Hsiao CH, Chang YC, et al. Percutaneous computed tomography-guided coaxial core biopsy for small pulmonary lesions with ground-glass attenuation. J Thorac Oncol 2012; 7:143–150. [CrossRef]

48. Shimizu K, Ikeda N, Tsuboi M, Hirano T, Kato H. Percutaneous CT-guided fine needle aspiration for lung cancer smaller than 2 cm and revealed by ground-glass opacity at CT. Lung Cancer 2006; 51:173–179. [CrossRef]

49. Yamagami T, Yoshimatsu R, Miura H, et al. Diagnostic performance of percutaneous lung biopsy using automated biopsy needles under CT-fluoroscopic guidance for ground-glass opacity lesions. Br J Radiol 2013; 86:20120447. [CrossRef]

50. Choo JY, Park CM, Lee NK, Lee SM, Lee HJ, Goo JM. Percutaneous transthoracic needle biopsy of small (≤1 cm) lung nodules under C-arm cone-beam CT virtual navigation guidance. Eur Radiol 2013; 23:712–719. [CrossRef]

51. Choi JW, Park CM, Goo JM, et al. C-arm cone-beam CT-guided percutaneous transthoracic needle biopsy of small (≤20 mm) lung nodules: diagnostic accuracy and complications in 161 patients. Am J Roentgenol 2012; 199:W322–330. [CrossRef]

52. Lee SM, Goo JM, Park CM, Lee HJ, Im JG. A new classification of adenocarcinoma: what the radiologists need to know. Diagn Interv Radiol 2012; 18:519–526.

53. Ikeda K, Nomori H, Mori T, et al. Impalpable pulmonary nodules with ground-glass opacity. Chest 2007; 131:502–506. [CrossRef]

54. Lee NK, Park CM, Kang CH, et al. CT-guided percutaneous transthoracic localization of pulmonary nodules prior to video-assisted thoracoscopic surgery using barium suspension. Korean J Radiol 2012; 13:694–701. [CrossRef]

55. Chen SF, Zhou JH, Zhang J, et al. Video-assisted thoracoscopic solitary pulmonary nodule resection after CT-guided hookwire localization: 43 cases report and literature review. Surg Endosc 2011; 25:1723–1729. [CrossRef]

56. Erickson LM, Shaw D, Macdonald FR. Prolonged barium retention in the lung following bronchography. Radiology 1979; 130:635–636.

57. Kwon WJ, Kim HJ, Jeong YJ, et al. Direct lipiodol injection used for a radio-opaque lung marker: stability and histopathologic effects. Exp Lung Res 2011; 37:310–317. [CrossRef]

58. Zaman M, Bilal H, Woo CY, Tang A. In patients undergoing video-assisted thoracoscopic surgery excision, what is the best way to locate a subcentimetre solitary pulmonary nodule in order to achieve successful excision? Interact Cardiovasc Thorac Surg 2012; 15:266–272. [CrossRef]

59. Nakao M, Yoshida J, Goto K, et al. Long-term outcomes of 50 cases of limited-resection trial for pulmonary ground-glass opacity nodules. J Thorac Oncol 2012; 7:1563–1566. [CrossRef]

60. Yang CFJ, D'Amico TA. Thoracoscopic segmentectomy for lung cancer. Ann Thorac Surg 2012; 94:668–681. [CrossRef]

61. Fukui T, Mitsudomi T. Small peripheral lung adenocarcinoma: clinicopathological features and surgical treatment. Surg Today 2010; 40:191–198. [CrossRef]

62. Harada H, Okada M, Sakamoto T, Matsuoka H, Tsubota N. Functional advantage after radical segmentectomy versus lobectomy for lung cancer. Ann Thorac Surg 2005; 80:2041–2045. [CrossRef]

63. Aoki T, Nakata H, Watanabe H, et al. Evolution of peripheral lung adenocarcinomas: CT findings correlated with histology and tumor doubling time. Am J Roentgenol 2000; 174:763–768. [CrossRef]

64. Kakinuma R, Ohmatsu H, Kaneko M, et al. Progression of focal pure ground-glass opacity detected by low-dose helical computed tomography screening for lung cancer. J Comput Assist Tomogr 2004; 28:17–23. [CrossRef]

65. Lindell RM, Hartman TE, Swensen SJ, et al. Five-year lung cancer screening experience: CT appearance, growth rate, location, and histologic features of 61 lung cancers. Radiology 2007; 242:555–562. [CrossRef]

66. Saito H, Yamada K, Hamanaka N, et al. Initial findings and progression of lung adenocarcinoma on serial computed tomography scans. J Comput Assist Tomogr 2009; 33:42–48. [CrossRef]

67. Matsuguma H, Mori K, Nakahara R, et al. Characteristics of subsolid pulmonary nodules showing growth during follow-up with CT scanning. Chest 2013; 143:436–443. [CrossRef]